



S-curve Motion Profile Design for Vibration Control of Single Link Flexible Manipulator

Tek Eksen Esnek Manipülâtörün Titreşim Kontrolü için S-eğrisi Hareket Profili Tasarımı

Murat Akdağ^{1*}, Hayrettin Şen²

¹ Dokuz Eylül University, Faculty of Engineering, Department of Mechanical Engineering, Izmir, TURKEY

² Dokuz Eylül University, The Graduate School of Natural and Applied Sciences, Izmir, TURKEY

Sorumlu Yazar / Corresponding Author*: murat.akdag@deu.edu.tr

Geliş Tarihi / Received: 03.11.2020

Araştırma Makalesi/Research Article

Kabul Tarihi / Accepted: 25.12.2020

DOI:10.21205/deufmd.2021236827

Atf şekli/How to cite: AKDAĞ M., ŞEN H. (2021). S-curve Motion Profile Design for Vibration Control of Single Link Flexible Manipulator. DEÜFMD 23(68), 661-676.

Abstract

In flexible manipulators, it is important the reduce end-effector vibrations. Suppression of end-effector vibrations significantly increases the precision of the performed work. Selection of velocity profile for giving motion to a manipulator is crucial to reduce the vibrations especially during high-speed motions. In this study, the effect of 3rd order S-curve velocity motion profile time parameters which is related with natural period of flexible manipulator on endpoint vibrations of a flexible beam are investigated. The S-curve motion profile results and trapezoidal motion profile results are also compared. The acceleration and deceleration times of both S-curve and trapezoidal velocity motion profiles are selected equal. Finite elements model of flexible robot manipulator is created and solution of the transient response under given velocity profile is obtained by using Newmark method. The results obtained from the Newmark method are compared with the results obtained from the model established using ANSYS program. The effects of time parameters of S-curve motion profiles on endpoint vibrations were shown by comparing in terms of amplitudes.

Keywords: S-curve Motion Profile, Vibration Control, Flexible Manipulator, Newmark Method

Öz

Esnek manipülâtörlerde, uç işlevcinin titreşimlerinin azaltılması önemlidir. Son uç işlevcinin titreşimlerinin bastırılması, yapılan işin hassasiyetini önemli ölçüde artırır. Bir manipülâtörü hareket ettirmek için gerekli hız profilinin seçimi, özellikle yüksek hızlı hareketler sırasında titreşimleri azaltmak için çok önemlidir. Bu çalışmada, esnek manipülâtörün doğal periyodu ile ilişkili 3. dereceden S-eğrisi hız hareket profili zaman parametrelerinin esnek bir kirişin uç nokta titreşimleri üzerindeki etkisi incelenmiştir. S-eğrisi hareket profili sonuçları ve trapez hareket profili sonuçları da karşılaştırılır. Hem S-eğrisi hem de trapez hız hareket profillerinin hızlanma ve yavaşlama süreleri eşit olarak seçilmiştir. Esnek robot manipülâtörünün sonlu elemanlar modeli oluşturulmuş ve verilen hız profili altındaki geçici rejim tepkisinin çözümü Newmark yöntemi kullanılarak elde edilmiştir. Newmark yönteminden elde edilen sonuçlar ANSYS programı kullanılarak oluşturulan modelden elde edilen sonuçlarla karşılaştırılır. S-eğrisi hareket profillerinin zaman parametrelerinin uç nokta titreşimleri üzerindeki etkileri, oluşan genlikler karşılaştırılarak gösterilmiştir.

Anahtar Kelimeler: S-eğrisi Hareket Profili, Titreşim Kontrolü, Esnek Manipülâtör, Newmark Metodu

1. Introduction

Serial manipulators are commonly used in industry for too many purposes such as pick and place, welding, path following applications etc. During their motion or working process the end effector vibration of the serial manipulator should be controlled. This control is achieved in a passive way by increasing the rigidity of the arms of the manipulators in industry. The weight of the arms is also increased via this rigidity. However, the amount of payload the robot can carry decreases. For this reason, the low weight serial flexible robots can be used to perform this type of tasks. Therefore, this type of robots can be actuated with low power motors. However, there is vibration problem of this type of manipulators. The flexible manipulators were defined as lightweight manipulators or they have large dimensions in the study [1]. Some literature reviews for dynamic analysis, design and control of flexible manipulators were also given in [2-4].

Ankaralı and Diken studied on the residual vibration problem of a flexible link manipulator which is actuated by cycloidal motion profile. In their study it is observed that at certain frequencies of the rise motion cause the zero-residual vibration [5]. Diken and Alghamdi did experiments on a rotating flexible aluminum beam in their study [6] to verify the simulation study of Ankaralı [5].

The basic velocity motion profile needed to actuate a serial manipulator is a trapezoidal velocity motion profile. Trapezoidal velocity profiles have three-time parameters as acceleration time, deceleration time and constant velocity time. Selection of these time parameters are important for suppression of end point vibrations of a flexible manipulator or to keep the end point vibrations at a certain level. Some studies [7, 8] showed that selection of the trapezoidal motion profile times which are related with the natural period of the one degree of freedom flexible manipulator, reduces the residual vibrations. The same approach was also applied two degree of freedom flexible manipulator and obtained the reduced residual vibrations in the study [9]. In these studies [7-9] selection of the deceleration time as an integer multiples of fundamental natural period of the flexible manipulator showed the residual vibration was suppressed.

In the literature, different velocity profiles were suggested to actuate a motor or dynamic system which is smoother than trapezoidal velocity motion profile due to the sharp acceleration changes in the trapezoidal velocity profiles. The firstly proposed the 3rd order S-curve motion profile which has seven-time segment by Castain and Paul [10] was used also in practice [11-14], since it has moderate complexity to use and enables minimum time motion with limited jerk.

For high precision requirements, higher order motion profiles were used due to the continues jerk profile [15]. In these studies [15, 16], 4th order S-curve motion profile which has fifteen time segment were selected and used. An algorithmic study was also proposed by Nguyen et. al. for designing a motion profile which has desired order [17]. In their study, a seven-segment velocity profile which has harmonic jerk model was also designed and it was shown that while the higher order motion profiles caused the less position error, the velocity profile which has harmonic jerk model caused the minimum position error.

In the study of Meckl and Arestides [18], dimensionless ramp up time of a 3rd order S-curve motion profile was calculated by using the acceleration time of a reference trapezoidal velocity motion profile and the natural frequency of a lightly-damped system. It was shown that in the simulation studies on a lightly-damped system, the proposed new 3rd order S-curve motion profile gave more suppressed residual vibration results than both trapezoidal velocity motion profile and 3rd order S-curve motion profile which has a ratio of 1/6 between ramp up time and acceleration time.

In the study of Li et al. [19] a three-segment motion profile which has a level-shifted cosinoidal acceleration function was proposed and experimental residual vibration results of a point to point linear motion under both the given trapezoidal velocity profile and the proposed motion profile were discussed. They also proposed [20] a developed seven-segment motion profile which has s-shape acceleration profile with a level-shifted sinusoidal form. The experimental results of point to point linear motion under the given input trapezoidal velocity motion profile, 3rd order S-curve motion profile and proposed seven-segment

motion profile were shown in terms of residual vibrations.

Byeogjin Kim et al. [21] studied the residual vibrations of an undamped system under the trigonometric and trapezoidal acceleration motion profiles. In their study the motion profiles were defined by the times for each segment. It was found that the zero vibration conditions were obtained if the selection of these time parameters for each segment as half-integer multiples of natural period for trigonometric profiles and integer-multiples for the trapezoidal acceleration profiles.

Fang et al. [22] proposed a fifteen-segment S-curve motion profile that has sigmoid jerk profile. Experimental residual vibration results of point to point motion for six-DOF manipulator were presented and it was observed that the results of proposed fifteen-segment sigmoid motion profile were better than both the given inputs trapezoidal velocity motion profile and 7th order S-curve motion profile.

In this study, it was shown that the trapezoidal and S-curve motion profile time parameters, which will minimize the residual vibration amplitudes of a flexible manipulator, should be related to the natural period of the system, according to other studies examined above. The trapezoidal and S-curve motion profiles created by considering these motion profile design parameters were compared. The effects of the trapezoidal and S-curve motion profile time parameters which are selected integer multiple of natural period of flexible manipulator on the residual vibration amplitudes were examined separately. This study was carried out for a flexible manipulator, which is a continuous system, unlike those that usually involve lumped mass systems. The acceleration and deceleration times of velocity motion profiles were selected equal for both trapezoidal and S-curve velocity motion profiles. Finite element model of flexible robot manipulator was created and solution of the transient response under given velocity profile was obtained by using Newmark method. The results obtained from the Newmark method are compared with the results obtained from the model established using ANSYS program. As a result of the performed studies, it has been shown that selecting the time parameters as twice as the natural period is effective in reducing the

transient and residual vibration amplitudes. It has been shown that the S-curve motion profile, which provides almost zero residual vibration amplitudes with appropriately selected parameters, always gives better results in terms of both transient and residual vibration amplitudes compared to the trapezoidal motion profile.

2. Analyses by MATLAB Code and ANSYS Based on Finite Element Theory

2.1. Finite element

A MATLAB code is developed based on the theory of the finite element method (FEM) [23]. The model of the one-link manipulator under study is shown in Figure 1 (a). Member-2 is the OB-beam. There is a revolute joint at O between Member-2 and the frame (Member-1). Member-2 is actuated by Motor-2 at O. The mass of Motor-2 is on the frame at O. There is a payload at B and a sensor at C on Member-2. The payload and sensor mass have a translational inertia of m_L and m_{sen} and rotational inertia of I_L and I_{sen} respectively.

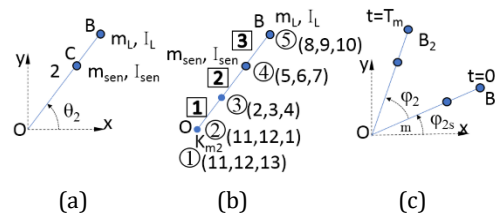


Figure 1. (a) Model (b) FE-model and (c) starting and stopping locations of the manipulator

The instantaneous angular position of Member-2 is $\theta_2(t)$, where t is the time. The length of the link is $L_2=OB$. The global origin is at O. The global Cartesian coordinates are x, y and z.

The finite element model (FEM) of the system is shown in Figure 1 (b). The number of finite elements for Member-2 is n_{e2} . For Figure 1 (b), $n_{e2}=3$. The number for n_e has been chosen as 3 for explanation. The model can be extended to different number of finite elements. The MATLAB code has been developed for any given n_{e2} .

The node numbers are shown in circles. The FE identification numbers are shown in squares. The plane frame analysis is considered, and each node has 3 degrees of freedom. The identification numbers of 3 displacements for

each node are given in the parentheses. For example, FE-2 has Node-3 at its origin and Node-4 at the far end. The displacements for Node-3 are d_{s2} , d_{s3} , and, d_{s4} , respectively. The local Cartesian coordinates of FE-2 are x_2 , y_2 and z_2 . The local origin of FE-2 is at Node-3 and x_2 axis is towards Node-4. The planar motion is considered, and thus z_2 axis is always parallel to z axis. The displacements in x and y directions for Node-3 are d_{s2} and d_{s3} , respectively. The flexural rotation of the cross-section for Node-3 is r_{s4} and $d_{s4}=h_2r_{s4}$, where h_2 is the length of FE-2. The instantaneous angle of orientation for x_2 is γ_3 , $\gamma_3= \theta_2$. Beam FE's and their parameters are shown in Table 1.

Table 1. FE- parameters

FE- Member	On Nodes	FE Nodes	Length	γ_n	Id. numbers for displacements at nodes
1	2	2,3	L_2/n_{e2}	θ_2	11,12,1,2,3,4
2	2	3,4	L_2/n_{e2}	θ_2	2,3,4,5,6,7
3	2	4,5	L_2/n_{e2}	θ_2	5,6,7,8,9,10

The theory of the FE analysis is given in many textbooks [23].The displacement (\mathbf{d}_{eln}), force (\mathbf{f}_{eln}), stiffness (\mathbf{k}_{eln}), and mass (\mathbf{m}_{eln}) matrices in local coordinates of a finite element (FE-n) are given below [7, 9, 23]. The node numbers are j at the local origin, and k at the far end of FE-n. Flexural bending is about the z axis.

$$\mathbf{d}_{eln} = \begin{Bmatrix} u_{jn} \\ v_{jn} \\ h_n r_{jn} \\ u_{kn} \\ v_{kn} \\ h_n r_{kn} \end{Bmatrix} \mathbf{m}_{eln} = \frac{\rho_n A_n h_n}{420} \begin{bmatrix} 140 & 0 & 0 & 70 & 0 & 0 \\ 0 & 156 & 22h_n & 0 & 54 & -13h_n \\ 0 & 22h_n & 4h_n^2 & 0 & 13h_n & -3h_n^2 \\ 70 & 0 & 0 & 140 & 0 & 0 \\ 0 & 54 & 13h_n & 0 & 156 & -22h_n \\ 0 & -13h_n & -3h_n^2 & 0 & -22h_n & 4h_n^2 \end{bmatrix} \quad (1)$$

$$\mathbf{k}_{eln} = \begin{bmatrix} \frac{A_n E_n}{h_n} & 0 & 0 & -\frac{A_n E_n}{h_n} & 0 & 0 \\ 0 & \frac{12E_n I_n}{h_n^3} & \frac{6E_n I_n}{h_n^2} & 0 & \frac{-12E_n I_n}{h_n^3} & \frac{6E_n I_n}{h_n^2} \\ 0 & \frac{6E_n I_n}{h_n^2} & \frac{4E_n I_n}{h_n} & 0 & \frac{-6E_n I_n}{h_n^2} & \frac{2E_n I_n}{h_n} \\ -\frac{A_n E_n}{h_n} & 0 & 0 & \frac{A_n E_n}{h_n} & 0 & 0 \\ 0 & \frac{-12E_n I_n}{h_n^3} & \frac{-6E_n I_n}{h_n^2} & 0 & \frac{12E_n I_n}{h_n^3} & \frac{-6E_n I_n}{h_n^2} \\ 0 & \frac{6E_n I_n}{h_n^2} & \frac{2E_n I_n}{h_n} & 0 & \frac{-6E_n I_n}{h_n^2} & \frac{4E_n I_n}{h_n} \end{bmatrix} \mathbf{f}_{eln} = \begin{Bmatrix} F_{jnx'} + q_{nx'} \frac{h_n}{2} \\ F_{jny'} + q_{ny'} \frac{h_n}{2} \\ T_{jn} + q_{ny'} \frac{h_n^2}{12} \\ F_{knx'} + q_{nx'} \frac{h_n}{2} \\ F_{kny'} + q_{ny'} \frac{h_n}{2} \\ T_{kn} + q_{ny'} \frac{h_n^2}{12} \end{Bmatrix} \quad (2)$$

Here, h_n is the length of FE-n. It has a uniform cross section and A_n is the cross-sectional area. The nodal displacement at Node- m in the x_n direction is u_{mn} , where $m=j$ or k . The nodal displacement in the y_n direction is v_{nm} . The flexural rotation of the cross section at Node- m is r_{mn} . The external load forces at Node- m in the x_n and y_n directions are $F_{mnx'}$ and $F_{mny'}$, respectively. The external bending moment at Node- m is T_{mn} . The distributed external loads on the FE-n in the x_n and y_n directions are $q_{nx'}$

and $q_{ny'}$, respectively. The modulus of elasticity is E_n , I_n is the bending moment of inertia of the cross section and ρ_n is the density.

The displacement (\mathbf{d}_{egn}), force (\mathbf{f}_{egn}), stiffness (\mathbf{k}_{egn}), and mass (\mathbf{m}_{egn}) matrices in global coordinates of FE-n are given below [23].

$$\mathbf{d}_{egn} = \mathbf{T}_n \mathbf{d}_{eln}, \mathbf{k}_{egn} = \mathbf{T}_n^T \mathbf{k}_{eln} \mathbf{T}_n \\ \mathbf{f}_{egn} = \mathbf{T}_n \mathbf{f}_{eln}, \mathbf{m}_{egn} = \mathbf{T}_n^T \mathbf{m}_{eln} \mathbf{T}_n \quad (3)$$

where, \mathbf{T}_n is the transformation matrix and \mathbf{T}_n^T is the transpose of \mathbf{T}_n . The transformation matrix is given as

$$\mathbf{T}_n = \begin{bmatrix} c_n & s_n & 0 & 0 & 0 & 0 \\ -s_n & c_n & 0 & 0 & 0 & 0 \\ 0 & 0 & 1 & 0 & 0 & 0 \\ 0 & 0 & 0 & c_n & s_n & 0 \\ 0 & 0 & 0 & -s_n & c_n & 0 \\ 0 & 0 & 0 & 0 & 0 & 1 \end{bmatrix} \quad (4)$$

$c_n = \cos\gamma_n, s_n = \sin\gamma_n$

Node-1 and Node-2 are coincident in Figure 1 (b), but their flexural rotations are different due to the revolute joint at O. There is a rotational spring between Node-1 and Node-2 (K_{m2}). The rotational spring K_{m2} is for Motor-2. There are masses representing the sensor and the payload at Node-4 and Node-5 respectively. The Node-1 is fixed. So, $d_{s11}=0$, $d_{s12}=0$, and $d_{s13}=0$. The reaction torque required to fix the rotation is provided by Motor-2.

The mathematical model of the system is obtained as

$$\mathbf{m}_s \ddot{\mathbf{d}}_s + \mathbf{c}_s \dot{\mathbf{d}}_s + \mathbf{k}_s \mathbf{d}_s = \mathbf{f}_s \quad (5)$$

Here, \mathbf{m}_s is the system mass matrix, \mathbf{c}_s is the system damping matrix, \mathbf{k}_s is the system stiffness matrix, \mathbf{d}_s is the system displacement matrix, and \mathbf{f}_s is the system force matrix. The sizes of \mathbf{d}_s and \mathbf{f}_s are 10×1 , and the sizes of \mathbf{m}_s , \mathbf{c}_s , and \mathbf{k}_s are 10×10 for the configuration in Figure 1 (b). For example, $\mathbf{d}_s(6,1)=d_{s6}$, which is the displacement of Node-4 in the y direction. $\mathbf{f}_s(6,1)=f_{s6}$, which is the external force at Node-4 in the y direction [7, 9].

Global FE matrices with a size of 6×6 are assembled to obtain the system stiffness (\mathbf{k}_s) and the mass (\mathbf{m}_s) matrices. For example,

$$\begin{aligned} \mathbf{k}_s(6,5) &= \mathbf{k}_{eg2}(5,4) + \mathbf{k}_{eg3}(2,1) \\ \mathbf{m}_s(6,5) &= \mathbf{m}_{eg2}(5,4) + \mathbf{m}_{eg3}(2,1) \end{aligned} \quad (6)$$

The combination of (6,5) exist in FE-2 and FE-3 as observed in Table 1. The combination of (6,5) is the combination of (5,4) for the FE-2 matrix, and the combination of (2,1) for FE-3 matrix.

Considering the kinetic energy, m_L and I_L are

added to the system mass matrix as the following [7, 9].

$$\begin{aligned} \mathbf{m}_s(5,5) &= \mathbf{m}_{eg2}(4,4) + m_{sen} \\ \mathbf{m}_s(6,6) &= \mathbf{m}_{eg2}(5,5) + m_{sen} \\ \mathbf{m}_s(7,7) &= \mathbf{m}_{eg2}(6,6) + I_{sen} \end{aligned} \quad (7)$$

$$\begin{aligned} \mathbf{m}_s(8,8) &= \mathbf{m}_{eg3}(4,4) + m_L \\ \mathbf{m}_s(9,9) &= \mathbf{m}_{eg3}(5,5) + m_L \\ \mathbf{m}_s(10,10) &= \mathbf{m}_{eg3}(6,6) + I_L \end{aligned} \quad (8)$$

Considering the potential energy, K_{m2} is added to the system stiffness matrix as the following [7, 9].

$$\mathbf{k}_s(1,1) = \mathbf{k}_{eg2}(3,3) + K_{m2} \quad (9)$$

2.1.1. Damping

The Rayleigh damping is considered as

$$\mathbf{c}_s = \eta \mathbf{m}_s + \beta \mathbf{k}_s \quad (10)$$

where, η and β are damping coefficients [24].

2.2. Newmark Method

The Newmark method [25] is used for the motion analysis. A time step, Δt , is chosen for the solution as $\Delta t < (T_{max}/20)$ where T_{max} is period for the highest natural frequency considered [9]. Knowing the solution at a time step, the solution at the subsequent time step is found by the numerical integration. The time step is given as $\Delta t = t_{n+1} - t_n$, where t_n and t_{n+1} are the successive time values. Let \mathbf{m}_n , \mathbf{c}_n , \mathbf{k}_n , \mathbf{d}_n , and \mathbf{f}_n be the system mass, damping, stiffness, nodal displacement and nodal force matrices (\mathbf{m}_s , \mathbf{c}_s , \mathbf{k}_s , \mathbf{d}_s , and \mathbf{f}_s) at the time step t_n . The Newmark solution is given as [9]. The numerical values of the model are given in Table 2.

$$\begin{aligned} [a_0 \mathbf{m}_{n+1} + a_1 \mathbf{c}_{n+1} + \mathbf{k}] \mathbf{d}_{n+1} &= \mathbf{f}_n \\ + \mathbf{m}_n [a_0 \mathbf{d}_n + a_2 \dot{\mathbf{d}}_n + a_3 \ddot{\mathbf{d}}_n] \\ + \mathbf{c}_n [a_1 \mathbf{d}_n + a_4 \dot{\mathbf{d}}_n + a_5 \ddot{\mathbf{d}}_n] \end{aligned} \quad (11)$$

$$\ddot{\mathbf{d}}_{n+1} = a_0 [\mathbf{d}_{n+1} - \mathbf{d}_n] - a_2 \dot{\mathbf{d}}_n - a_3 \ddot{\mathbf{d}}_n \quad (12)$$

$$\dot{\mathbf{d}}_{n+1} = \dot{\mathbf{d}}_n + a_6 \ddot{\mathbf{d}}_n + a_7 \ddot{\mathbf{d}}_{n+1} \quad (13)$$

where

$$\begin{aligned}
 a_0 &= \frac{1}{\alpha \Delta t^2}, a_1 = \frac{\delta}{\alpha \Delta t}, a_2 = \frac{1}{\alpha \Delta t}, \\
 a_3 &= \frac{1}{2\alpha} - 1, a_4 = \frac{\delta}{\alpha} - 1, a_5 = \frac{\Delta t}{2} \left(\frac{\delta}{\alpha} - 2 \right) \\
 a_6 &= \Delta t(1 - \delta), a_7 = \delta \Delta t, \\
 \alpha &= \frac{1}{4}(1 + \gamma)^2, \delta = \frac{1}{2} + \gamma
 \end{aligned}
 \tag{14}$$

2.2. Modeling the manipulator in ANSYS

Finite element model of flexible beam was created in Ansys and transient response of the beam under the given velocity motion profile was observed. BEAM188 element type which has two nodes was used in order to model the manipulator. Two-point mass were included in model as accelerometer and payload mass. The modeled manipulator was shown in Figure 2. The model properties of the manipulator were given on Table 2.

Table 2. Model Properties of the manipulator

Elastic modulus	2.1x10 ¹¹ Pa
Poisson ratio	0.3
Density	7800 kg/m ³
Accelerometer mass	54 gr
Inertia of the accelerometer	9.18450x10 ⁻⁶ kgm ²
Payload mass	130.69 gr
Inertia of payload	1.49564x10 ⁻⁵ kgm ²
Cross section	1.95x40.6 mm ²
Beam length (L ₂)	300 mm
Acc. Position from the origin	266 mm
Rayleigh damping coefficients	η=0 and β=2x10 ⁻⁴
Newmark amp. decaying factor	γ = 0.005
Motor rotational spring constant	K _{m2} =16000 Nm/rad
Number of finite elements	ne2=150
Time step	Δt=0.005 s

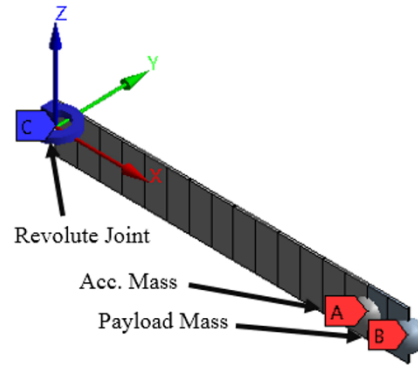


Figure 2. Created model in ANSYS

3. S-curve Motion Profile Design

Trapezoidal velocity profile design for desired motion angle and motion time parameters which are T_{acc} , T_{cons} and T_{dec} shown in Figure 3 (a) were given in the studies [7-9]. Selection of the T_{dec} time as integer multiple of the fundamental period of the manipulator was proved that the residual vibrations were suppressed significantly [7-9]. In this study, seven-segment 3rd order polynomial S-curve motion profile were used in order to actuate a one-DOF flexible manipulator. The S-curve motion profile and all-time parameters are shown in Figure 3 (b). The acceleration and deceleration times of velocity motion profiles were selected equal. In order to design the motion profile all time parameters and travel distance were given as inputs. By using these inputs maximum velocity and acceleration values were calculated.

Motion profile was designed for point to point motion in seven segments, each segment takes a time interval of T_i , $i=1,2,3...7$. Total motion time T_m is summation of all seven-time intervals. For the symmetrical motion profile, $T_1=T_3=T_5=T_7$ and $T_2=T_6$. Then total motion time can be defined as $T_m=4T_1+2T_2+T_4$. All these time parameters and a trapezoidal velocity motion profile were shown in Figure 3. In order to design the S-curve motion profile T_m , D_{max} which is total motion angle and all-time intervals ($T_{1,2,3...7}$) were given as inputs.

At an arbitrary time t , the equations of acceleration, velocity and angular displacement at a specific time interval were expressed as follows. The final values of velocity and angular position at a specific phase were also given to calculate the A_{max} .

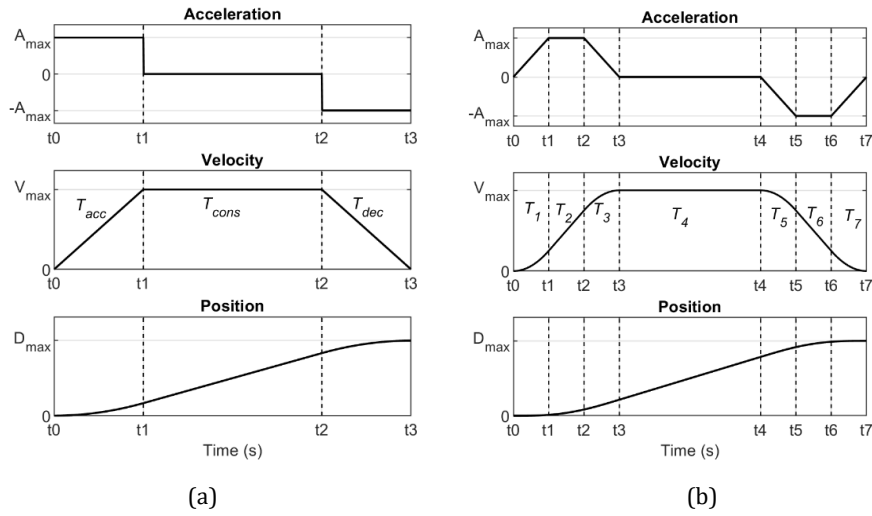


Figure 3. (a) Trapezoidal Velocity Motion Profile (b) 3rd order S-curve Motion Profile

For $t \in [t_0, t_1]$,

$$a(t) = A_{max} \frac{t}{T_1} \quad (15)$$

$$v(t) = A_{max} \frac{t^2}{2T_1} \rightarrow V_1 = A_{max} \frac{T_1}{2} \quad (16)$$

$$d(t) = A_{max} \frac{t^3}{6T_1} \rightarrow D_1 = A_{max} \frac{T_1^2}{6} \quad (17)$$

For $t \in [t_1, t_2]$,

$$a(t) = A_{max} \quad (18)$$

$$v(t) = V_1 + A_{max}(t - t_1) \quad (19)$$

$$V_2 = V_1 + A_{max}T_2$$

$$d(t) = D_1 + V_1(t - t_1) + A_{max} \frac{(t - t_1)^2}{2} \quad (20)$$

$$D_2 = D_1 + V_1T_2 + A_{max} \frac{T_2^2}{2}$$

For $t \in [t_2, t_3]$,

$$a(t) = A_{max} - A_{max} \frac{(t - t_2)}{T_3} \quad (21)$$

$$v(t) = V_2 + A_{max}(t - t_2) - A_{max} \frac{(t - t_2)^2}{2T_3} \quad (22)$$

$$V_{max} = V_3 = V_2 + A_{max} \frac{T_3}{2}$$

$$d(t) = D_2 + V_2(t - t_2) + A_{max} \frac{(t - t_2)^2}{2} - A_{max} \frac{(t - t_2)^3}{6T_3}, D_3 = D_2 + V_2T_3 + A_{max} \frac{T_3^2}{3} \quad (23)$$

For $t \in [t_3, t_4]$,

$$a(t) = 0 \quad (24)$$

$$v(t) = V_{max} \rightarrow V_4 = V_{max} \quad (25)$$

$$d(t) = D_3 + V_{max}(t - t_3), D_4 = D_3 + V_{max}T_4 \quad (26)$$

For $t \in [t_4, t_5]$,

$$a(t) = -A_{max} \frac{(t - t_4)}{T_5} \quad (27)$$

$$v(t) = V_{\max} - A_{\max} \frac{(t-t_4)^2}{2T_5} \quad (28)$$

$$V_5 = V_{\max} - A_{\max} \frac{T_5}{2}$$

$$d(t) = D_4 + V_{\max}(t-t_4) - A_{\max} \frac{(t-t_4)^3}{6T_5} \quad (29)$$

$$D_5 = D_4 + V_{\max}T_5 - A_{\max} \frac{T_5^2}{6}$$

For $t \in [t_5, t_6]$,

$$a(t) = -A_{\max} \quad (30)$$

$$v(t) = V_5 - A_{\max}(t-t_5) \rightarrow V_6 = V_5 - A_{\max}T_6 \quad (31)$$

$$d(t) = D_5 + V_5(t-t_5) - A_{\max} \frac{(t-t_5)^2}{2} \quad (32)$$

$$D_6 = D_5 + V_5T_6 - A_{\max} \frac{T_6^2}{2}$$

For $t \in [t_6, t_7]$,

$$a(t) = A_{\max} \frac{(t-t_6)}{T_7} - A_{\max} \quad (33)$$

$$v(t) = V_6 - A_{\max}(t-t_6) + A_{\max} \frac{(t-t_6)^2}{2T_7} \quad (34)$$

$$V_7 = 0 = V_6 - A_{\max} \frac{T_7}{2}$$

$$d(t) = D_6 + V_6(t-t_6) - A_{\max} \frac{(t-t_6)^2}{2} + A_{\max} \frac{(t-t_6)^3}{6T_7}, \quad D_7 = D_6 + V_6T_7 - A_{\max} \frac{T_7^2}{3} \quad (35)$$

$$D_{\max} = A_{\max}(T_1 + T_2)(2T_1 + T_2 + T_4) \quad (36)$$

From Eq. (36) value of A_{\max} can be calculated since D_{\max} and all-time parameters ($T_{1,2,3...7}$) were given as inputs. The only unknown parameter is A_{\max} for all equations. After obtaining the value of A_{\max} from Eq. (36), for all acceleration, velocity

and position values can be calculated for all time steps of desired motion time.

4. The effect of S-curve motion profile time parameters on the transient and residual vibrations

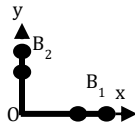
In the study of the Byeogjin Kim et al. [21] it was shown that the selection of the 3rd order polynomial S-curve motion profile time parameters as integer multiple of the natural period of an undamped two degree of freedom system cause the zero residual vibrations. The given motion cases in Table 3 will be performed, in order to observe the effects of the S-curve motion time parameters on the transient and residual vibrations of designed flexible manipulator which has properties given in Table 2. The same approach in the study of Byeogjin Kim et al. [21] were also taken into consideration during the design of the motion cases in order to observe whether it works on also a multi-DOF damped system or not.

The acceleration and deceleration times of motion profiles were selected equally. The 3rd order motion profile time parameters were defined by the vector $\mathbf{qs}_m = [T_1, T_2, T_3, T_m]$. The simulations were performed same total motion angle θ_m which is D_{\max} and same time motion which is T_m . T_m is selected as 22t1h for motion cases. Total analysis time was defined as $T_{\text{res}}=2s$ in order to observe the residual vibrations for all performed analysis. t1h is the time which is half of the fundamental natural period of the manipulator.

The vibration responses of the both Ansys and Newmark solution are given in Figure 4 for the comparison. It is seen that the Newmark solution very well fit the Ansys solution from Figure 4 (a) and (b). Since the residual response differences between the Ansys and Newmark solution are in the scale of micrometers, this amount of differences can be acceptable. After this verification only the results of Newmark solution will be presented.

After these obtained results the comparison between analyses results of proposed trapezoidal velocity motion profiles [7-9] and analyses results of the selection of the S-curve motion time parameters as integer multiple of the natural period of flexible manipulator will be presented in the Chapter 5 in detail.

Table 3. Motion cases for S-curve velocity motion profiles

Case-1/ S-curve	$[\theta_s \theta_m]$	$T_m - T_{res}$	Schematic	t1h (Newmark)	t1h(ANSYS)
[3.25t1h, 3.5t1h, 3.25t1h, T_m]	[0, 90]	1.32s-2s		1/8.3331/2	1/8.3329/2
[3t1h, 4t1h, 3t1h, T_m]				$\approx 0.06s$	$\approx 0.06s$
[4t1h, 3t1h, 4t1h, T_m]					
[4t1h, 2t1h, 4t1h, T_m]					

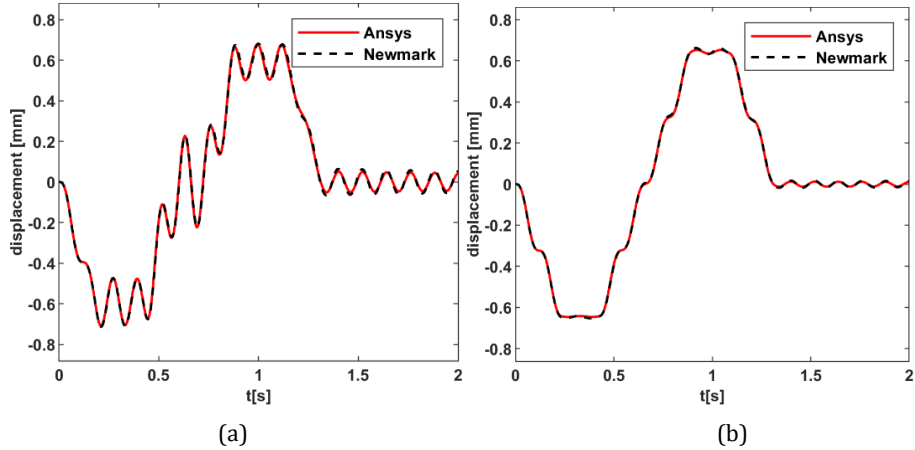


Figure 4. Vibration response comparison between Ansys and Newmark solution for Case 1 $q_{sm}=[3t1h, 4t1h, 3t1h, T_m]$ for (a), $q_{sm}=[4t1h, 3t1h, 4t1h, T_m]$ for (b)

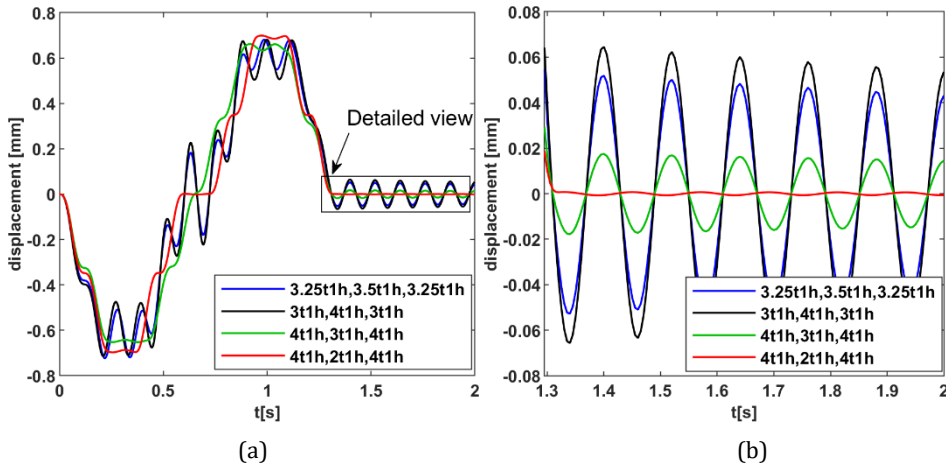


Figure 5. (a) Transient and residual vibrations responses for all motions of Case-1 (b) detailed view of residual vibrations

Table 4. Numerical results of the performed analyses Case-1

Case-1	V_{max} (rad/s)	A_{max} (rad/s ²)	Max. Amp. (mm)	Max. Res. Amp. (μm)
[3.25t1h, 3.5t1h, 3.25t1h, T_m]	2.1817	5.3868	0.7233	52.7136
[3t1h, 4t1h, 3t1h, T_m]	2.1817	5.1944	0.7148	65.6206
[4t1h, 3t1h, 4t1h, T_m]	2.38	5.6667	0.662	17.7858
[4t1h, 2t1h, 4t1h, T_m]	2.1817	6.0602	0.6989	0.7295

5. The Comparison of Trapezoidal and S-curve Motion Profiles Results

In this study, comparison of the transient response results between the proposed trapezoidal velocity motion profiles [7-9] and 3rd order S-curve motion profile were also investigated. The selection of the time parameters of trapezoidal motion profile as integer multiple of the natural period of flexible manipulator were reduced the residual vibrations significantly in [7-9]. In order compare the transient response results acceleration, deceleration and motion times of the trapezoidal motion profile were selected equal to 3rd order motion profile acceleration, deceleration and motion times. The acceleration and deceleration times of motion

profiles were also selected equally. The 3rd order motion profile time parameters were defined by the vector $\mathbf{q}_{s_m} = [T_1, T_2, T_3, T_m]$ as mentioned before. The motion time parameters of trapezoidal velocity profile were defined by the vector $\mathbf{q}_{t_m} = [T_{acc}, T_{cons}, T_{dec}, T_m]$. The simulations were performed same total motion angle θ_m which is D_{max} and different time motion which is T_m . The calculated time parameters for trapezoidal motion profile was indicated with "*" in \mathbf{q}_{t_m} . All motion cases for transient analyses were given in Table 5. Total analysis time was defined as $T_{res}=2s$ in order to observe the residual vibrations for all performed analysis. t_{1h} is the time which is half of the fundamental natural period of the manipulator.

Table 5. Motion Cases for both S-curve motion profiles and Trapezoidal motion profiles

Cases	$[\theta_s \theta_m]$	T_m - T_{res}	Schematic	t1h (Newmark)	t1h (ANSYS)
Case-2					
S-curve	Trapezoidal				
[2t1h,0,2t1h, T_m]	[4t1h,12t1h,4t1h, T_m]				
[2t1h,2t1h,2t1h, T_m]	[6t1h,8t1h,6t1h, T_m]				
[2t1h,4t1h,2t1h, T_m]	[8t1h,4t1h,8t1h, T_m]				
[2t1h,6t1h,2t1h, T_m]	[10t1h,0,10t1h, T_m]	[0,90]		1.2s-2s	
[4t1h,0,4t1h, T_m]	[8t1h,4t1h,8t1h, T_m]				
[4t1h,2t1h,4t1h, T_m]	[10t1h,0,10t1h, T_m]				
				1/8.3331/2	1/8.3329/2
Case-3					
S-curve	Trapezoidal			$\approx 0.06s$	$\approx 0.06s$
[2t1h,0,2t1h, T_m]	[4t1h,*,4t1h, T_m]				
[2t1h,2t1h,2t1h, T_m]	[6t1h,*,6t1h, T_m]	[0,90]	1s-2s		
[2t1h,4t1h,2t1h, T_m]	[8t1h,*,8t1h, T_m]				
[4t1h,0,4t1h, T_m]	[8t1h,*,8t1h, T_m]				
Case-4					
S-curve	Trapezoidal				
[2t1h,0,2t1h, T_m]	[4t1h,0,4t1h, T_m]	[0,90]	0.48s-2s		

The motion profiles in Case-2 have 1.2s motion time and all-time parameters of motion profiles both S-curve and trapezoidal ones are selected as integer multiple of natural period of flexible manipulator. In Case-3 motion profiles have 1s

motion time and the time parameters except T_4 and T_{cons} are selected as integer multiple of natural period of the manipulator. In Case-4 the S-curve motion profile is designed in order to perform the same job of Case-2 and Case-3 in

shortest time. The time parameters T_2 , T_4 and T_1 are selected as zero, zero and one natural period of the flexible manipulator respectively in Case-4.

The vibration response results under the given motion profiles for Case-2 $qs_m=[2t1h,6t1h,2t1h, T_m]$ and $qt_m=[10t1h,0,10t1h,T_m]$ are shown in Figure 6 (a). The maximum deflections for the transient region and residual region are also shown in Figure 6 (a) and (b) respectively. Similarly the vibration responses for given motion profiles for Case-3 $qs_m=[2t1h,2t1h,2t1h, T_m]$ and $qt_m=[6t1h,*,6t1h,T_m]$ are also shown in Figure 6 (c). The detailed view in Figure 6 (c) and maximum deflections for residual vibrations are given in Figure 6 (d). The maximum deflection values and the amount of the amplitude reductions in percentage for both transient and residual regions are given in Table 6 and Table 7 The reached maximum velocity and acceleration values are also included in Table 6 and Table 7.

In order to make a better comparison between the trapezoidal and S-curve motion profiles results the reached maximum velocities for both motion profiles were selected the same by defining the same acceleration and deceleration times for both motion profiles. Although the S-curve motion profiles has higher acceleration values, the vibration results seem to be better than the trapezoidal velocity motion profiles in terms of both transient and residual vibrations for all motion cases in Case-2 according to given data in Table 6 The existence and amount of T_2 causes less maximum transient vibration amplitudes even if the acceleration times are selected equally such as between the results of $qs_m=[2t1h,4t1h,2t1h,T_m]$ and

$qs_m=[4t1h,0,4t1h,T_m]$ for both Case-2 and Case-3 and $qs_m=[2t1h,6t1h,2t1h,T_m]$ and $qs_m=[4t1h,2t1h,4t1h,T_m]$ for Case-2. When the S-curve motion profiles which have the same acceleration times were investigated, the usage only T_1 in the acceleration time without using T_2 causes the high acceleration values and high transient vibration amplitudes. For this reason, T_1 should be selected as short as possible and T_2 can be selected as any integer multiple of natural period of the flexible manipulator depending on T_m . All the time parameters of the motion profiles in Case-2 were selected integer multiple of natural period of the manipulator for both trapezoidal and S-curve motion profile. When the all-time parameters both for S-curve and trapezoidal motion profiles are selected as integer multiple of natural period of the manipulator or zero, the maximum residual vibration amplitudes do not vary from one motion profile to another one that can be seen from Table 6.

The effects of T_4 and T_{cons} not being chosen as the integer multiple of the natural period on the vibration results are shown in Table 7 for the motion profiles of Case-3. While it is observed that the fact that T_4 is not an integer multiple of the natural period has no effect on the vibration results, it is understood that the fact that T_{cons} is not an integer multiple of the natural period has an important effect on the residual vibration results. The trapezoidal motion profile gave the almost same result with a few differences for the minimum motion time in Case-4. The S-curve motion profiles maximum residual vibration amplitudes is related with both reached maximum velocity and acceleration values as shown in both Table 6 and Table 7.

Table 6. Results of Case-2

Case-2										
S-curve	Trapezoidal	V_{max} (rad/s) qs_m and qt_m	A_{max} (rad/s ²)		%Max Amp. Reduction	%Max Residual Amp. Reduction	Max. Amp. (mm)		Max. Res. Amp. (µm)	
			qs_m	qt_m			qs_m	qt_m	qs_m	qt_m
[2t1h,0,2t1h,T _m]	[4t1h,12t1h,4t1h,T _m]	1.636	13.6	6.82	1.164	96.15	1.568	1.586	1.08	28.13
[2t1h,2t1h,2t1h,T _m]	[6t1h,8t1h,6t1h,T _m]	1.87	7.79	5.19	27.14	97.09	0.898	1.233	0.83	28.38
[2t1h,4t1h,2t1h,T _m]	[8t1h,4t1h,8t1h,T _m]	2.182	6.06	4.55	36.49	96.85	0.6995	1.102	0.90	28.66
[2t1h,6t1h,2t1h,T _m]	[10t1h,0,10t1h,T _m]	2.618	5.45	4.36	41.61	95.75	0.631	1.08	1.23	28.83
[4t1h,0,4t1h,T _m]	[8t1h,4t1h,8t1h,T _m]	2.182	9.09	4.55	5.003	96.42	1.046	1.102	1.03	28.66
[4t1h,2t1h,4t1h,T _m]	[10t1h,0,10t1h,T _m]	2.618	7.27	4.36	22.28	95.23	0.84	1.08	1.37	28.83

Table 7. Results of Case-3 and Case-4

Case-3										
S-curve	Trapezoidal	V_{max} (rad/s) q_{sm} and q_{tm}	A_{max} (rad/s ²)		%Max Amp. Reduction	%Max Residual Amp. Reduction	Max. Amp. (mm)		Max. Res. Amp. (μ m)	
			q_{sm}	q_{tm}			q_{sm}	q_{tm}	q_{sm}	q_{tm}
[2t1h,0,2t1h, T_m]	[4t1h,*,4t1h, T_m]	2.067	17.2	8.61	-2.32	98.1	1.979	1.934	2.61	137.3
[2t1h,2t1h,2t1h, T_m]	[6t1h,*,6t1h, T_m]	2.454	10.2	6.82	23.13	98.81	1.177	1.531	1.99	166.8
[2t1h,4t1h,2t1h, T_m]	[8t1h,*,8t1h, T_m]	3.021	8.39	6.29	31.62	98.89	0.967	1.414	2.35	211.5
[4t1h,0,4t1h, T_m]	[8t1h,*,8t1h, T_m]	3.021	12.6	6.29	-2.37	98.78	1.447	1.414	2.59	211.5
Case-4										
[2t1h,0,2t1h, T_m]	[4t1h,0,4t1h, T_m]	6.545	54.5	27.3	1.728	2.563	6.374	6.486	91.8	94.23

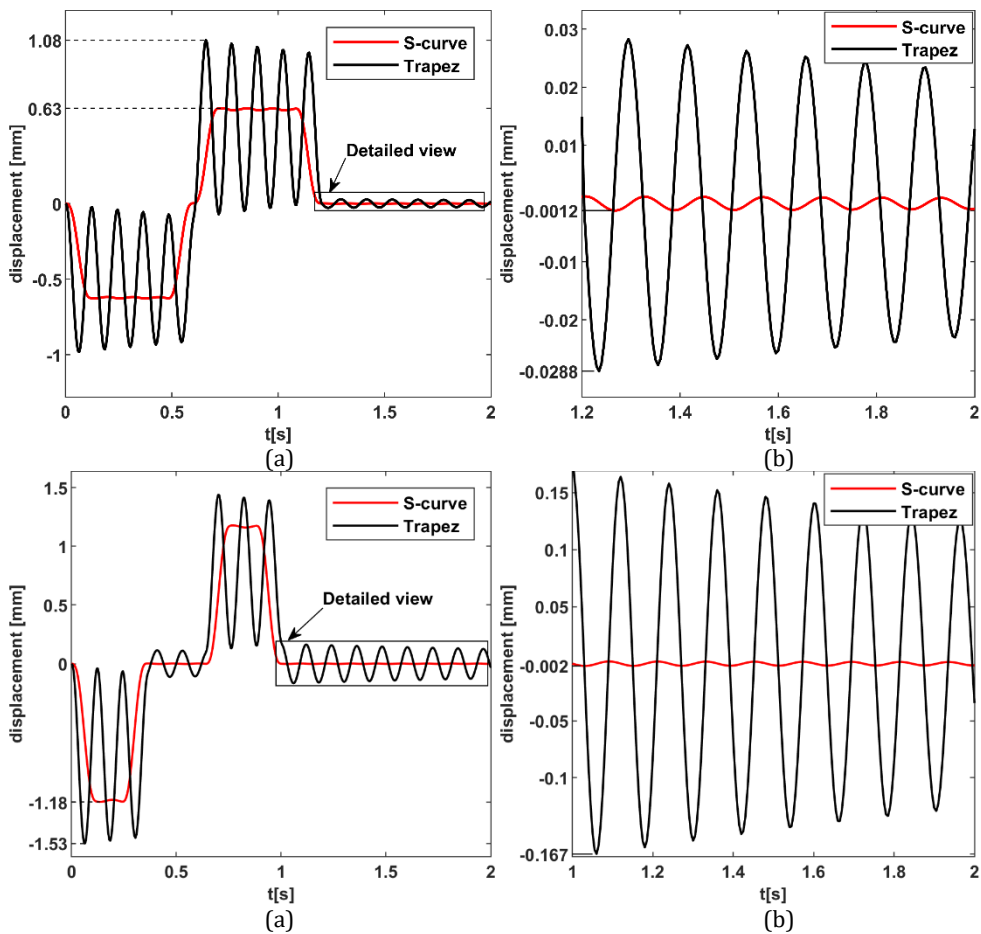


Figure 6. Vibration responses (a) for Case-2 $q_{sm}=[2t1h,6t1h,2t1h,T_m]$ and $q_{tm}=[10t1h,0,10t1h,T_m]$ (b) Detailed view of residual vibration of (a), (c) for Case-3 $q_{sm}=[2t1h,2t1h,2t1h,T_m]$ and $q_{tm}=[6t1h,*,6t1h,T_m]$ (d) Detailed view of residual vibration of (c)

The change of amplitudes in the results of the S-curve motion profiles from one motion to another one is less than the trapezoidal motion

profile results in terms of maximum residual amplitudes for motion Case-3. The selection of T_{cons} is effective on this result. In order to

investigate the effect of selection of T_4 and T_{cons} on the residual vibrations new motion profiles are designed and shown in Table 8. The effect of T_2 on the both residual and transient vibration amplitudes were explained as mentioned before. In design of Case-5 motion profiles given

in Table 8 for both S-curve and trapezoidal motion profiles the acceleration and deceleration times are selected equally, and the S-curve motion profiles has 4t1h second as T_2 time parameters. T_4 and T_{cons} time parameters are selected from 0 to 4t1h.

Table 8 Motion Cases for the investigation of the effect of the selection of T_4 and T_{cons} on residual vibrations

Case-5		T_m-T_{res}	$[\theta_s \theta_m]$	Schematic	t1h (simulation)	t1h (ANSYS)
S-curve	Trapezoidal				1/8.3331/2	1/8.3329/2
[2t1h,4t1h,2t1h, T_m]	[8t1h,0,8t1h, T_m]	0.96s-2s			$\approx 0.06s$	$\approx 0.06s$
[2t1h,4t1h,2t1h, T_m]	[8t1h,*,8t1h, T_m]	0.98s-2s				
[2t1h,4t1h,2t1h, T_m]	[8t1h,*,8t1h, T_m]	1s-2s				
[2t1h,4t1h,2t1h, T_m]	[8t1h,t1h,8t1h, T_m]	1.02s-2s				
[2t1h,4t1h,2t1h, T_m]	[8t1h,*,8t1h, T_m]	1.04s-2s				
[2t1h,4t1h,2t1h, T_m]	[8t1h,*,8t1h, T_m]	1.06s-2s				
[2t1h,4t1h,2t1h, T_m]	[8t1h,2t1h,8t1h, T_m]	1.08s-2s				
[2t1h,4t1h,2t1h, T_m]	[8t1h,*,8t1h, T_m]	1.1s-2s				
[2t1h,4t1h,2t1h, T_m]	[8t1h,*,8t1h, T_m]	1.12s-2s				
[2t1h,4t1h,2t1h, T_m]	[8t1h,3t1h,8t1h, T_m]	1.14s-2s				
[2t1h,4t1h,2t1h, T_m]	[8t1h,*,8t1h, T_m]	1.16s-2s				
[2t1h,4t1h,2t1h, T_m]	[8t1h,*,8t1h, T_m]	1.18s-2s				
[2t1h,4t1h,2t1h, T_m]	[8t1h,4t1h,8t1h, T_m]	1.2s-2s				

Table 9. The results of Case-5 motion cases

Case-5											
S-curve	Trapezoidal	T_m-T_{res} (sec.)	V_{max} (rad/s)	A_{max} (rad/s ²)		%Max Amp. Reducti on	%Max Res. Reducti on	Max. Amp. (mm)		Max. Res. Amp. (μ m)	
				q_{s_m}	q_{t_m}			q_{s_m}	q_{t_m}	q_{s_m}	q_{t_m}
[2t1h,4t1h,2t1h, T_m]	[8t1h,0,8t1h, T_m]	0.96-2	3.27	9.09	6.82	36.62	88.66	1.053	1.661	3.548	31.293
[2t1h,4t1h,2t1h, T_m]	[8t1h,*,8t1h, T_m]	0.98-2	3.14	8.73	6.55	31.41	97.45	1.008	1.47	2.956	115.82
[2t1h,4t1h,2t1h, T_m]	[8t1h,*,8t1h, T_m]	1-2	3.02	8.39	6.29	31.62	98.89	0.967	1.414	2.347	211.54
[2t1h,4t1h,2t1h, T_m]	[8t1h,t1h,8t1h, T_m]	1.02-2	2.91	8.08	6.06	31.65	99.2	0.93	1.361	1.99	247.88
[2t1h,4t1h,2t1h, T_m]	[8t1h,*,8t1h, T_m]	1.04-2	2.81	7.79	5.84	33.48	99.13	0.899	1.352	1.905	218.2
[2t1h,4t1h,2t1h, T_m]	[8t1h,*,8t1h, T_m]	1.06-2	2.71	7.52	5.64	37.35	98.63	0.87	1.388	1.852	134.85
[2t1h,4t1h,2t1h, T_m]	[8t1h,2t1h,8t1h, T_m]	1.08-2	2.62	7.27	5.45	36.57	94.28	0.841	1.325	1.704	29.794
[2t1h,4t1h,2t1h, T_m]	[8t1h,*,8t1h, T_m]	1.1-2	2.53	7.04	5.28	31.52	98.24	0.812	1.186	1.547	87.998
[2t1h,4t1h,2t1h, T_m]	[8t1h,*,8t1h, T_m]	1.12-2	2.45	6.82	5.11	31.67	99.06	0.785	1.148	1.545	164.5
[2t1h,4t1h,2t1h, T_m]	[8t1h,3t1h,8t1h, T_m]	1.14-2	2.38	6.61	4.96	31.68	99.2	0.761	1.114	1.564	195.94
[2t1h,4t1h,2t1h, T_m]	[8t1h,*,8t1h, T_m]	1.16-2	2.31	6.42	4.81	33.13	99.18	0.74	1.106	1.435	175.07
[2t1h,4t1h,2t1h, T_m]	[8t1h,*,8t1h, T_m]	1.18-2	2.24	6.23	4.68	37.05	98.95	0.72	1.143	1.171	111.76
[2t1h,4t1h,2t1h, T_m]	[8t1h,4t1h,8t1h, T_m]	1.2-2	2.18	6.06	4.55	36.49	96.85	0.7	1.102	0.903	28.656

The results of Case-5 motion profiles are given in Table 9. When the T_1 and T_2 are selected as integer multiple of natural period of the flexible manipulator, the selection of T_4 either as any multiple of natural period of the manipulator or zero does not affect the maximum residual vibration amplitudes according to given data in Table 9. The maximum residual vibration amplitudes of S-curve motion profiles results are decreased linearly by the increasing the T_4 which causes the decrement of both reached maximum velocity and acceleration values. The increment of T_{cons} does not cause linearly decrement on the maximum residual vibration amplitudes of the trapezoidal motion profile results. It can be seen in Table 9 the minimum residual vibration amplitudes for trapezoidal

motion profiles are occurred when the T_{cons} are selected as integer multiple of natural period of the manipulator. The effects of T_4 and T_{cons} on the maximum residual vibration amplitudes are shown in Figure 7 (a) and (b) for both trapezoidal and S-curve motion profiles respectively.

Therefore, all time parameters of trapezoidal motion profiles should be selected as integer multiple of natural period of the manipulator in order to obtain minimum residual vibration amplitudes. In order to obtain minimum residual vibration amplitudes under an S-curve motion profile input the time parameters except T_4 should be selected as integer multiple of natural period of the manipulator.

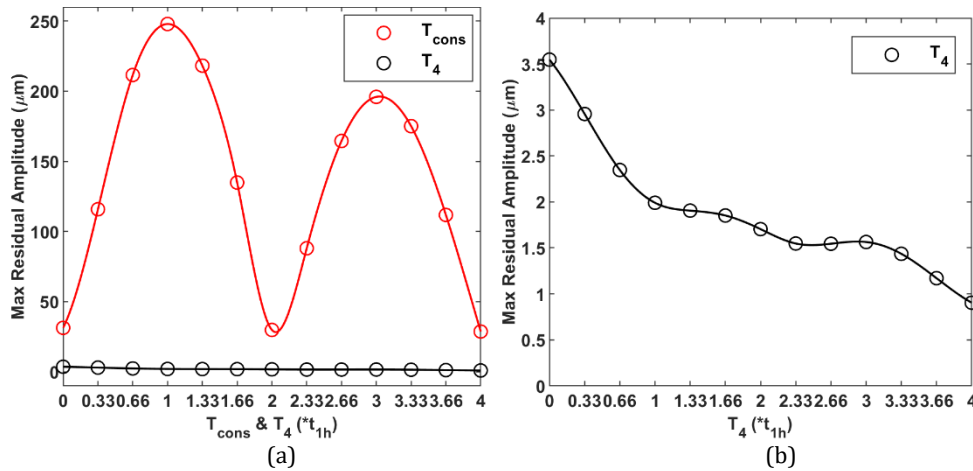


Figure 7. Max. Residual vibration amplitudes (a) effect of T_4 (b) effect of T_{cons}

6. Conclusions

In this study the effect of the S-curve motion time parameters on the transient and residual vibrations of a flexible manipulator were investigated. When the time parameters of S-curve motion profile were defined as integer multiple of natural period of flexible manipulator, the residual vibrations were reduced effectively. The comparison between the results of S-curve motion profiles and trapezoidal motion profiles were also investigated for different motion cases. The S-curve motion profiles gave better results than trapezoidal motion profiles in terms of residual vibration amplitudes, even if they reach the same maximum velocity and the S-curve motion profiles reach higher acceleration values than trapezoidal motion profiles. It is found that the

existence of T_2 which is the S-curve motion time parameter causes the less maximum transient vibration amplitudes when the results of S-curve motion profiles which have the same acceleration time were compared. It was obtained that for S-curve motion profiles the selection of T_4 as any multiple of the natural period of the flexible manipulator or zero does not affect the residual vibration amplitudes. However, the selection of T_{cons} as integer multiple of the natural period of the flexible manipulator is crucial in order to reduce the residual vibration amplitudes. In order to obtain minimum residual vibration amplitudes, all the time parameters of the trapezoidal motion profile should be selected as integer multiple of natural period of the flexible manipulator, while the S-curve motion profile time parameters except T_4 should be selected as

integer multiple of natural period of the manipulator according to the obtained results. In terms of residual vibration amplitudes, it was observed that the motion profiles which have time parameters as integer multiple of natural period of the manipulator do not have a significant advantage compared to each other. This conclusion is valid for both S-curve and trapezoidal motion profiles. However, the acceleration time should be selected as long as possible for both S-curve and trapezoidal motion profiles in terms of transient vibration amplitudes. In order to obtain the minimum transient vibration amplitudes for S-curve motion profiles T_1 should be selected minimum as $2t_{1h}$ and T_2 should be selected as long as possible depending on T_m . The T_{acc} and T_{dec} times should be selected as long as possible and T_{cons} should be selected as short as possible in order to obtain less transient vibration amplitudes for trapezoidal motion profiles.

References

- [1] Gao, Y., et al., 2012, Flexible Manipulators: Modeling, Analysis and Optimum Design. Academic Press, 260. DOI: 10.1016/C2011-0-07379-9.
- [2] Benosman, M. and G. Le Vey, 2004, Control of Flexible Manipulators: A Survey, *Robotica*, Volume. 22(5), p. 533-545. DOI: 10.1017/S0263574703005642.
- [3] Dwivedy, S.K. and P. Eberhard, 2006, Dynamic Analysis of Flexible Manipulators, a Literature Review, *Mechanism and machine theory*, Volume. 41(7), p. 749-777. DOI: 10.1016/j.mechmachtheory.2006.01.014.
- [4] Sayahkarajy, M., Z. Mohamed, and A.A. Mohd Faudzi, 2016, Review of Modelling and Control of Flexible-Link Manipulators, *Proceedings of the Institution of Mechanical Engineers, Part I: Journal of Systems and Control Engineering*, Volume. 230(8), p. 861-873. DOI: 10.1177/0959651816642099.
- [5] Ankarali, A. and H. Diken, 1997, Vibration Control of an Elastic Manipulator Link, *Journal of Sound and Vibration*, Volume. 204(1), p. 162-170. DOI: 10.1006/jsvi.1996.0897.
- [6] Diken, H. and A. Alghamdi, 2003, Residual Vibration Response Spectra for a Servomotor-Driven Flexible Beam, *Proceedings of the Institution of Mechanical Engineers, Part C: Journal of Mechanical Engineering Science*, Volume. 217(5), p. 577-583. DOI: 10.1243/095440603765226867.
- [7] Malgaca, L., et al., 2016, Residual Vibration Control of a Single-Link Flexible Curved Manipulator, *Simulation Modelling Practice and Theory*, Volume. 67, p. 155-170. DOI: 10.1016/j.simpat.2016.06.007.
- [8] Yavuz, S., L. Malgaca, and H. Karagülle, 2016, Vibration Control of a Single-Link Flexible Composite Manipulator, *Composite Structures*, Volume. 140, p. 684-691. DOI: 10.1016/j.compstruct.2016.01.037.
- [9] Karagülle, H., et al., 2017, Vibration Control of a Two-Link Flexible Manipulator, *Journal of Vibration and Control*, Volume. 23(12), p. 2023-2034. DOI: 10.1177/1077546315607694.
- [10] Castain, R.H. and R.P. Paul, 1984, An on-Line Dynamic Trajectory Generator, *The International Journal of Robotics Research*, Volume. 3(1), p. 68-72. DOI: 10.1177/027836498400300106.
- [11] Liu, C. and Y. Chen, 2018, Combined S-Curve Feedrate Profiling and Input Shaping for Glass Substrate Transfer Robot Vibration Suppression, *Industrial Robot: the international journal of robotics research and application*, Volume. 45(4), p. 549-560. DOI: 10.1108/ir-11-2017-0201.
- [12] Liu, S. 2002, An on-Line Reference-Trajectory Generator for Smooth Motion of Impulse-Controlled Industrial Manipulators, *IEEE, 7th International Workshop on Advanced Motion Control. Proceedings (Cat. No. 02TH8623)*, 3-5 July, Maribor, Slovenia, p. 365-370. DOI: 10.1109/AMC.2002.1026947.
- [13] Lu, T.-C. and S.-L. Chen, 2016, Genetic Algorithm-Based S-Curve Acceleration and Deceleration for Five-Axis Machine Tools, *The International Journal of Advanced Manufacturing Technology*, Volume. 87(1-4), p. 219-232. DOI: 10.1007/s00170-016-8464-0.
- [14] Mu, H., et al., 2008, Third-Order Trajectory Planning for High Accuracy Point-to-Point Motion, *Frontiers of Electrical and Electronic Engineering in China*, Volume. 4(1), p. 83-87. DOI: 10.1007/s11460-009-0017-y.
- [15] Boryga, M. and A. Graboś, 2009, Planning of Manipulator Motion Trajectory with Higher-Degree Polynomials Use, *Mechanism and Machine Theory*, Volume. 44(7), p. 1400-1419. DOI: 10.1016/j.mechmachtheory.2008.11.003.
- [16] Lambrechts, P., M. Boerlage, and M. Steinbuch, 2005, Trajectory Planning and Feedforward Design for Electromechanical Motion Systems, *Control Engineering Practice*, Volume. 13(2), p. 145-157. DOI: 10.1016/j.conengprac.2004.02.010.
- [17] Nguyen, K.D., T.-C. Ng, and I.-M. Chen, 2008, On Algorithms for Planning S-Curve Motion Profiles, *International Journal of Advanced Robotic Systems*, Volume. 5(1), p. 11. DOI: 10.5772/5652.
- [18] Meckl, P.H. and P.B. Arestides. 1998, Optimized S-Curve Motion Profiles for Minimum Residual Vibration, *IEEE, Proceedings of the 1998 American Control Conference. ACC (IEEE Cat. No. 98CH36207)*, 26-26 June, Philadelphia, PA, USA, p. 2627-2631. DOI: 10.1109/ACC.1998.688324.
- [19] Li, H., et al. 2006, A New Motion Control Approach for Jerk and Transient Vibration Suppression, *IEEE, 2006 4th IEEE International Conference on Industrial Informatics*, 16-18 Aug., Singapore, p. 676-681. DOI: 10.1109/INDIN.2006.275642.
- [20] Li, H., et al., 2009, Motion Profile Design to Reduce Residual Vibration of High-Speed Positioning Stages, *IEEE/ASME Transactions On Mechatronics*, Volume. 14(2), p. 264-269. DOI: 10.1109/TMECH.2008.2012160.
- [21] Kim, B., H.H. Yoo, and J. Chung, 2017, Robust Motion Profiles for the Residual Vibration Reduction of an Undamped System, *Journal of Mechanical Science*

- and Technology, Volume. 31(10), p. 4647-4656. DOI: 10.1007/s12206-017-0911-9.
- [22] Fang, Y., et al., 2019, Smooth and Time-Optimal S-Curve Trajectory Planning for Automated Robots and Machines, Mechanism and Machine Theory, Volume. 137, p. 127-153. DOI: 10.1016/j.mechmachtheory.2019.03.019.
- [23] Bathe, K., 2014, Finite Element Procedures, 2nd ed., USA: Prentice Hall, Person Education, Inc, 1065.
- [24] W. T. Thomson, M.D.D., 1988, Theory of Vibration with Applications, 3rd ed. Englewood Cliffs, Prentice-Hall, 500.
- [25] Newmark, N.M., 1959, A Method of Computation for Structural Dynamics, Journal of the engineering mechanics division, Volume. 85(3), p. 67-94. DOI: 10.1061/JMCEA3.0000098.